

Article

Particle-Mediated Gene Transfection and Organotypic Culture of Postmortem Human Retina

Rania A. Masri^{1,2}, Sammy C. S. Lee^{1,2}, Michele C. Madigan^{1,3}, and Ulrike Grünert^{1,2}

¹ The University of Sydney, Faculty of Medicine and Health, Save Sight Institute and Discipline of Ophthalmology, Sydney, Australia

² Australian Research Council Centre of Excellence for Integrative Brain Function, Sydney Node, The University of Sydney, Sydney, Australia

³ School of Optometry and Vision Science, University of New South Wales, Sydney, Australia

Correspondence: Ulrike Grünert, Save Sight Institute, 8 Macquarie St, Sydney, NSW 2000, Australia. e-mail: ulrike.grunert@sydney.edu.au

Received: 30 October 2018

Accepted: 7 January 2019

Published: 27 March 2019

Keywords: human retina; organotypic culture; retinal ganglion cells; particle mediated gene transfer

Citation: Masri RA, Lee SCS, Madigan MC, Grünert U. Particle-mediated gene transfection and organotypic culture of postmortem human retina. *Trans Vis Sci Tech.* 2019;8(2):7. <https://doi.org/10.1167/tvst.8.2.7> Copyright 2019 The Authors

Purpose: Particle-mediated gene transfer has been used in animal models to study the morphology and connectivity of retinal ganglion cells. The aim of the present study was to apply this method to transfect ganglion cells in postmortem human retina.

Methods: Postmortem human eyes from male and female donors aged 40 to 76 years old were obtained within 15 hours after death. In addition, two marmoset retinas were obtained immediately after death. Ganglion cells were transfected with an expression plasmid for the postsynaptic density 95 protein conjugated to green or yellow fluorescent protein. Retinas were cultured for 3 days, fixed and then processed with immunohistochemical markers to reveal their stratification in the inner plexiform layer.

Results: The retinas maintained their morphology and immunohistochemical properties for at least 3 days in culture. Bipolar and ganglion cell morphology was comparable to that observed in noncultured tissue. The quality of transfected cells in human retina was similar to that in freshly enucleated marmoset eyes. Based on dendritic field size and stratification, at least 11 morphological types of retinal ganglion cell were distinguished.

Conclusions: Particle-mediated gene transfer allows efficient targeting of retinal ganglion cells in cultured postmortem human retina.

Translational Relevance: The translational value of this methodology lies in the provision of an *in vitro* platform to study structural and connectivity changes in human eye diseases that affect the integrity and organization of cells in the retina.

Introduction

The organotypic culture of mammalian retina has provided an efficient model for the study of retinal biology,^{1–4} disease therapy,⁵ and pathophysiology.^{6–9} Retinal explants can be targeted with gene promoters and viral vectors and have the advantage over single-cell cultures that neural networks are preserved. In the past decade, the development of organotypic human retinal cultures has provided the opportunity to record from and manipulate intact human retina. Human *ex vivo* retinas have been transfected with adeno-associated viruses for application in gene therapy¹⁰ and optogenetic studies.^{11,12} Additionally,

human retinal explants have been used to test the effects of neurotoxic insult on ganglion cells¹³ and to study retinal degeneration patterns.¹⁴ In recent studies, organotypic culture has been combined with the use of biolistics in order to introduce transgenes to retinal neurons. This method has been applied to murine,^{15,16} rabbit,² and marmoset monkey^{17–20} retinas but to date has only been applied to fetal human retinal tissue.²¹ The aim of the present study was to use particle-mediated gene transfer in postmortem human retina in order to enable studies of retinal ganglion cells and their connectivity. Particle-mediated gene transfection provides a reliable way of manipulating transgenic expression in cultured hu-

Table 1. Donor Retinas Processed for Organotypic Culture and Particle Mediated Gene Transfection

ID	Eye	Sex	Age, y	Death to Enucleation, h	Enucleation to Medium, h ^a	Time in Medium, h	Cultured with RPE, Y/N	Time in Culture, h	Number of Analyzed Ganglion Cells
15155	R	M	58	10	1	2	N	67	57
15233	R	F	40	5	3	1	N	68	4
15373	L	M	66	1	3	9	N	88	18
15512	L	M	47	1	4	1	Y	68	58
15583	L	F	62	5	1	4	Y	87	10

^a The medium was Hibernate-A for #15155; and CO₂ Independent Medium for the other retinas; all retinas were placed in Ames' medium for at least 30 minutes before culture.

man retinal tissue in vitro within days. Here we combined biolistic labeling with immunohistochemistry using markers that would be useful in the analysis of ganglion cell connectivity in the inner plexiform layer.

Methods

Postmortem Donor Tissue

Postmortem human eyes from adult donors with no known history of eye disease were obtained from the Lions NSW Eye Bank (Sydney Eye Hospital) with consent and ethical approval from The University of Sydney Human Research Ethics Committee (HREC# 2012/2833); the protocols adhered to the Declaration of Helsinki. [Tables 1](#) and [2](#) summarize the information on donor eyes. Eyes were placed in Hibernate-A-Medium (Gibco, Thermo Fisher Scientific, North Ryde, NSW, Australia) or CO₂ Independent Medium (Gibco) at the Eye Bank. Subsequently, posterior eye cups were immersed for 30 minutes in oxygenated Ames' medium (Sigma-Aldrich, St. Louis, MO) containing 100 U/mL penicillin, 100 µg/mL streptomycin, and 0.292 mg/mL L-glutamine (Gibco), supplemented with 0.5% normal horse serum (Anti-

bodies Australia, Clayton, VIC, Australia). The eye cups were gently squeezed outside from the optic nerve downward to detach the vitreous humor. Retinas were dissected in supplemented Ames' medium in sterile conditions and cut into four to six pieces ([Fig. 1](#)). Each retinal piece was halved into a central and peripheral portion (maximum 10 × 15 mm) and cultured separately. The retinal pigment epithelium was retained in two experiments ([Table 1](#)) for co-culture with the retina.^{22,23}

Noncultured retinas used for comparison were initially fixed in the eye cup prior ($n = 1$) or after ($n = 3$) vitreous removal in 2% or 4% paraformaldehyde (PFA; [Table 2](#)) in 0.1 M phosphate buffer (PB), pH 7.4, rinsed in PB and then dissected.

Pieces from cultured and noncultured retinas intended for immunohistochemistry were immersed in 30% sucrose overnight in 0.1 M PB, frozen in liquid nitrogen, and kept at -80°C until use.

Marmoset Tissue

Two retinas were obtained from one male adult marmoset (*Callithrix jacchus*, aged 1.8 years). The animal was obtained from the Australian National Health and Medical Research Council's (NHMRC)

Table 2. Noncultured Donor Retinas

ID	Eye	Sex	Age, y	Death to Enucleation, h	Enucleation to Medium, h ^a	Time in Medium, h	Death to Fixation, h	Time in Fixative, h	Concentration of Fixative, % PFA
13587	R	F	44	2	N/A	N/A	4	12	2%
13699	R	M	56	2	N/A	N/A	9	21	2%
15022	R	M	69	9	5	14	33	1	4%
15054	R	F	76	9	2	11	30	1	4%

^a The medium used was Hibernate-A. Retinas #15022 and #15054 were also immersed in carboxygenated Ames' medium for 1 hour before fixation.

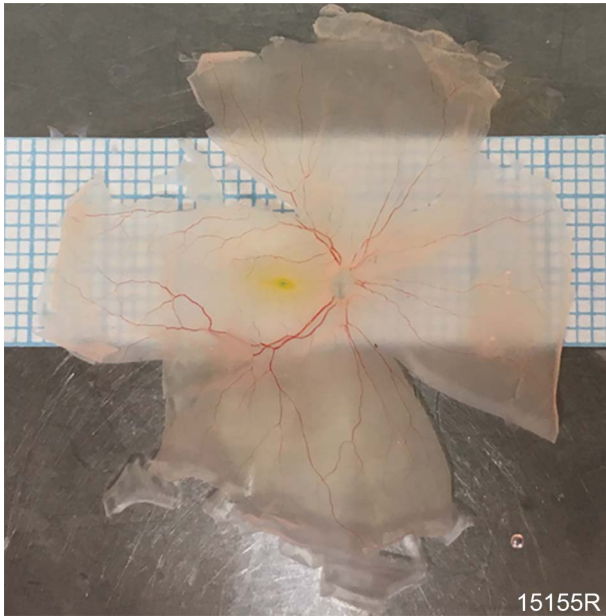


Figure 1. Micrograph of a freshly dissected human retina. The dissection was performed in Ames' medium and relieving cuts were made to flatten the retina. The macula (yellow) and surrounding blood vessels are visible. One-millimeter grid paper pictured for scale.

combined breeding facility. All procedures were carried out according to the provisions of the NHMRC Code of Practice for the Care and Use of Animals, were in compliance with the ARVO Statement for the Use of Animals in Ophthalmic and Vision Research, and were approved by the Animal Ethics Committee of The University of Sydney (AEC #558).

The marmoset was sedated with an intramuscular injection of 12 mg/kg Alfaxan (Jurox, Rutherford, NSW, Australia) and 3 mg/kg diazepam (Roche, NSW, Australia) and then euthanized with an overdose of sodium pentobarbitone (Letho-barb, Virbac, Milperra, NSW, Australia). The animal was transcardially perfused using 500 mL chilled sucrose-based solution consisting of 205 mM sucrose, 2.5 mM KCL, 26 mM NaHCO₃, 1.2 mM NaH₂PO₄·H₂O, 0.1 mM CaCl₂, 5 mM MgCl₂, 6H₂O, and 10 mM D-glucose.²⁴ The eyes were enucleated, dropped into 3% povidone-iodine solution in phosphate-buffered saline (PBS), rinsed with sterile PBS, and kept on ice in freshly made Ames' medium for a maximum of 45 minutes. The eyes were then immersed in oxygenated Ames' medium (95%O₂/5%CO₂) for 30 minutes. The anterior portion of the eye cup was removed, and the eye was gently squeezed from the optic nerve downward to remove the vitreous humor. The retina was dissected out of the eye cup and cut into four quadrants.

Particle-Mediated Gene Transfer and Organotypic Culture

The protocol for organotypic culture and gene transfection is a modification of a previously published protocol.^{2,17} Each retinal piece was flattened ganglion cell side up onto a 0.4- μ m pore size Millicell cell culture insert (30 mm diameter, Millipore, Temecula, CA). Excess medium was removed using filter paper in order to enable the retina to adhere to the membrane. A Helios gene gun system (Bio-Rad, Hercules, CA) was used to propel gold microcarriers into the tissue. The gold microcarriers (1.6 μ m diameter) were coated with a cytomegalovirus (CMV) postsynaptic density 95-green fluorescent protein (PSD95-GFP) fusion plasmid in a ratio of 1.5 μ g plasmid/1 mg gold (gift from Masaki Fukata, National Institute for Physiological Science, Osaka, Japan). Plasmids conjugated to yellow fluorescent protein (PSD95-YFP, gift from Rachel Wong, University of Washington, Seattle, WA) were used in one case (#15233). Bullets used within 2 months of preparation yielded optimal expression of the protein. The bullets were delivered at 100 psi. Retinas were shot through the filter of Transwell membrane cell culture inserts (3 μ m pore size membrane, 12 mm insert, Corning, Sigma-Aldrich) at a distance of \sim 50 mm. Initially, a modified gene gun barrel was used for retina #15155 at 40 mm distance from the tissue.²⁵ However, we found the original gun barrel to be less damaging to the retina and to provide a better distribution of the bullets. The Millicell inserts were fitted onto custom printed filter stands and placed in a tissue culture dish (100 \times 20 mm, Falcon, Corning, NY). The retinal pigment epithelium (if retained) was positioned at the base of the tissue culture dish.²² Dishes were filled with supplemented Ames' medium so that the photoreceptor side was in contact with the medium and the ganglion cell side was exposed to the atmosphere.² The entire chamber was placed in an incubator (37°C/ 5% CO₂; MCO-18M, SANYO, Osaka, Japan) and the retina cultured for 67 to 89 hours (Table 1). The medium was replaced daily.

After culture, the retinal pieces were removed from the incubator and the medium was replaced with 4% PFA in 0.1 M PB. Pieces were fixed for 1 hour. After rinses in 0.1 M PB, the pieces were processed for immunohistochemistry attached to the Millicell filter membrane, unless otherwise indicated.

Immunohistochemistry

Pieces from one cultured retina (#15233) were peeled off the filter membrane and used to cut vertical cryostat sections (Leica CM 3050 S) at a thickness of 14 μm . Sections were preincubated for 30 minutes in 5% normal donkey serum (NDS; Jackson ImmunoResearch Laboratories, Inc., West Grove, PA) in PBS containing 0.5% Triton X-100 (BDH Chemicals, Kilsyth, Australia). Primary antibodies (see Table 3) were diluted in 0.5% Triton X-100 in PBS and 0.05% NaN_3 with 3% NDS and applied overnight. Secondary antibodies were donkey anti-mouse, anti-rabbit, or anti-goat immunoglobulins (IgG) coupled to Alexa 594 or Alexa 488 (Jackson ImmunoResearch Laboratories, Inc.). The sections were coverslipped using Mowiol (Hoechst Australia Ltd., VIC, Australia) containing 10% DABCO (1,4-diazabicyclo [2.2.2]-octane; Sigma-Aldrich).

Other pieces from cultured (#15155; #15233; #15512) and noncultured retinas (Table 2) were processed free floating. The tissue was processed as described above except for that the incubation in primary antibodies was at 4°C for 4 to 7 days and that 10 $\mu\text{g}/\text{mL}$ DAPI (1:1000, 4',6-diamidino-2-phenylindole dihydrochloride, D9542, Sigma-Aldrich) was added to the secondary antibody diluent. Some retinal pieces were incubated in antibodies against green fluorescent protein in order to enhance GFP labeling. The tissue was flat mounted onto poly-lysine coated microscope slides and coverslipped with Vectashield mounting medium (Vector Laboratories, Inc., Burlingame, CA).

Microscopy

Tissue was imaged using a Zeiss Axioplan microscope (Zeiss, Oberkochen, Germany) or a confocal scanning microscope (Zeiss LSM700) equipped with 405, 488, 555, and 635 nm lasers at a resolution of 2048 \times 2048 pixels. Stacks of images were obtained at 0.5- to 1- μm increments using a 20 \times objective (Plan Aplanachromat no. 420650-9901) or a 40 \times water immersion objective (Plan Aplanachromat no. 421767-9970). The brightness and contrast of the images was adjusted in Zen Blue software (Zeiss) software or Adobe Photoshop CS6 (San Jose, CA).

Analysis

The dendritic field size of ganglion cells was measured from stacks of images using Fiji²⁶ as described previously.²⁰ The eccentricity of ganglion cells was calculated from low-power montages of the

retinal pieces. Stratification of ganglion cell dendrites was determined using orthogonal projections in Zen Blue, relative to the DAPI nuclear staining at the borders of the inner plexiform layer and/or to the stratification of calbindin labeled diffuse bipolar DB3a cells,^{27,28} recoverin labeled flat midget bipolar cells,²⁹ and ChAT labeled starburst amacrine cells.³⁰ Some retinal ganglion cells were reconstructed using the filament tracer in Imaris (Bitplane, Zurich, Switzerland) software.

Results

Preservation of Gross Morphology and Retinal Architecture

Retinas to be used for organotypic culture (Fig. 1) were checked to be in good condition after dissection, in particular we checked macroscopically that the photoreceptor layer was intact and did not peel off. Retinas co-cultured with the retinal pigment epithelium adhered more strongly to the filter membrane and were thus better preserved but this was not investigated systematically.

The main aim of the present study was to establish biolistic transfection in postmortem human retina but in order to check whether the transfected and cultured retinal tissue appeared qualitatively normal we compared noncultured and cultured retinas. A more quantitative analysis was not carried out as it would require comparison of tissue at the exact same eccentricity, the same age, and the same postmortem delay. This was beyond the scope of the present study.

Vertical cryostat sections or retinal flat mounts were processed with established immunohistochemical markers for neurons and Müller cells.^{27,29,31,32} Figures 2A–E show images of vertical sections through a cultured retina processed with these markers. The retinal layers are intact, but the inner and outer segments of the photoreceptors were damaged when the tissue pieces were peeled off the filter membrane. The appearance of glutamine synthetase labeled Müller cells (Fig. 2A), recoverin labeled flat midget bipolar cells (Figs. 2B, 2C), Islet-1 positive ON bipolar cells (Fig. 2B), and calretinin labeled amacrine cells (Fig. 2D) resembles previously published data of normal human retina.^{27,29,31,32} The dendritic terminals of PKC labeled rod bipolar cells are clearly visible in Figure 2D, but rod bipolar somas and axons were only weakly labeled. Figure 2E shows a vertical section labeled with antibodies against the ganglion cell marker RNA-binding protein with

Table 3. Antibodies

Antibody Name	Immunogen	Source, Catalogue Number, RRID	Antibody Type	Dilution
Calbindin (CaBP)	Recombinant rat calbindin D-28k	Swant, CB38, lot: 5.5 RRID: AB_10000340	Rabbit polyclonal	1:20,000
Calretinin (CaR)	Produced against recombinant human calretinin	Swant, 7699/4, lot: 1\$.1; RRID: AB_10000321	Goat polyclonal	1:5000
Choline acetyl transferase (ChAT)	Purified human placental choline acetyltransferase enzyme	Millipore, AB144P, lot: NG1780580; RRID: AB_2079751	Goat polyclonal	1:200
C-terminal binding protein (CtBP2)	Amino acids 361-445 of mouse C-terminal binding protein 2	BD Biosciences, 612044; RRID: AB_399431	Mouse monoclonal	1:10,000
Green fluorescent protein (GFP)	Green fluorescent protein isolated directly from the jellyfish <i>Aequorea victoria</i>	Thermo Fisher Scientific, A-6455, lot: 1692915; RRID: AB_221570	Rabbit polyclonal	1:1000
Green fluorescent protein	Derived from the jellyfish <i>Aequorea victoria</i> . Immunogen is a fusion protein corresponding to full length amino acid sequence 246	Rockland Immunochemicals, 600101215, RRID: AB_218182	Goat polyclonal	1:500
Glutamine synthetase	Human glutamine synthetase amino acids 1-373; recognizes band of 45 kDa	BD Transduction Laboratories, 610518; RRID: AB_2313767	Mouse monoclonal	1:6000
Islet-1	C-terminal portion of rat Islet-1	Developmental Studies Hybridoma Bank, 39.3F7; RRIDAB_1157901	Mouse monoclonal	1:250
Melanopsin	N-terminal peptide of human melanopsin protein (Liao et al. 2016)	King-Wai Yau, Johns Hopkins University School of Medicine, Baltimore, MD	Rabbit polyclonal	1:500
RBPMs	Recombinant protein encompassing a sequence within the center region of human RBPMs	Gene Tex, Sapphire Bioscience, GTX118619, lot: 40415; RRID: AB_10720427	Rabbit polyclonal	1:500
Recoverin	Recombinant human recoverin, recognizes one band of 26 kDa	Millipore, AB5585, lot: LV1480447; RRID: AB_2253622	Rabbit polyclonal	1:10,000

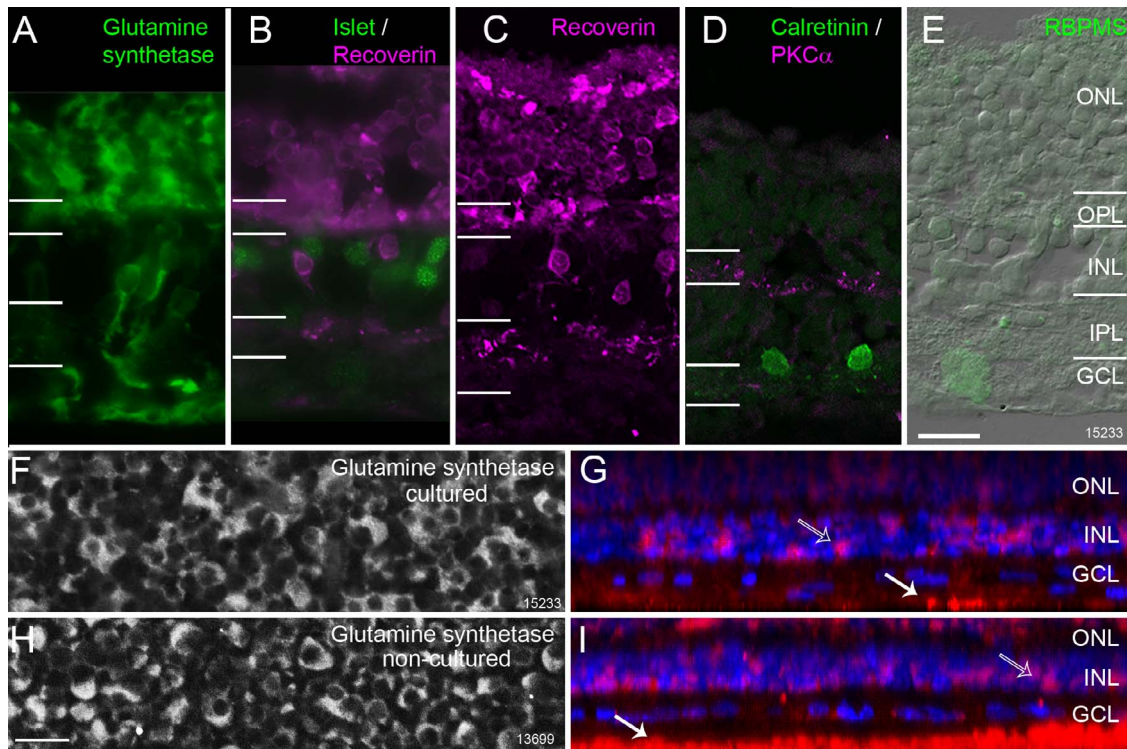


Figure 2. Organotypically cultured human retinas maintain their structure and immunohistochemical properties. (A) to (E) Conventional fluorescence micrographs (A, B) and confocal images (C–E) of vertical cryostat sections through cultured human retina. (A) Immunoreactivity for glutamine synthetase is present in Müller cell somas, end-feet, and processes. (B, C) Recoverin immunoreactivity (*magenta*) is present in photoreceptors and OFF midget bipolar cells, ON bipolar cell somas express Islet (*green*). (D) Calretinin is localized to amacrine cells in the inner nuclear layer, and PKC α is localized to rod bipolar cells whose dendrites are more strongly labeled. (E) RBPMS (*green*) is restricted to ganglion cells. Nomarski optics reveals the retinal layers (ONL, outer nuclear layer; OPL, outer plexiform layer; INL, inner nuclear layer; IPL, inner plexiform layer; GCL, ganglion cell layer). (F–I) Single confocal images of retinal flat mounts showing expression of glutamine synthetase by Müller cell bodies in cultured (F) and noncultured flat mount retina (H). The images in G and I are orthogonal projections of images stacks from the preparations shown in F and H, respectively, with glutamine synthetase shown in *red* and DAPI-labeled nuclei shown in *blue*. Scale bar shown in E = 20 μ m, applies to A–E; scale bar shown in H = 20 μ m (applies to F–I).

multiple splicing (RBPMS).^{33,34} Consistent with previous studies, expression of RBPMS was restricted to the somas of ganglion cells.

Flat mount preparations of cultured (Figs. 2F, 2G) and noncultured retinas (Figs. 2H, 2I) showed comparable expression of the Müller cell marker glutamine synthetase. Similarly, the morphology of bipolar and amacrine cells resembled that shown in previous studies of human retina.^{27,30} Figure 3 shows examples of calbindin and recoverin labeled bipolar somas and axon terminals in noncultured (Figs. 3A, 3B, 3E, 3F) and cultured (Figs. 3C, 3D, 3G, 3H) retinas, as well as ChAT expression in ON starburst somas and processes of noncultured (Figs. 3I, 3J) and cultured (Figs. 3K, 3L) retinas. Taken together, our results show that cells in postmortem human retina maintained their morphology and immunohistochemical properties after 3 days of organotypic culture.

Particle-Mediated Gene Transfection of Retinal Ganglion Cells

In both marmoset and human, a variety of retinal ganglion cell types were labeled using particle-mediated gene transfection (see below). Transfected cells are characterized by brightly labeled puncta distributed along the dendritic tree. The quality of the PSD95-GFP labeling in marmoset retina was superior to that found in human retina where the puncta were more irregular with respect to their size and distribution on the dendrites (see below). Nonetheless our results show that ganglion cells in postmortem human retina can express PSD95-GFP.

Figure 4 demonstrates the punctate appearance of PSD95-GFP labeling on the dendrites of retinal ganglion cells in marmoset (Fig. 4A, inset) and human (Fig. 4B). These puncta are thought to be

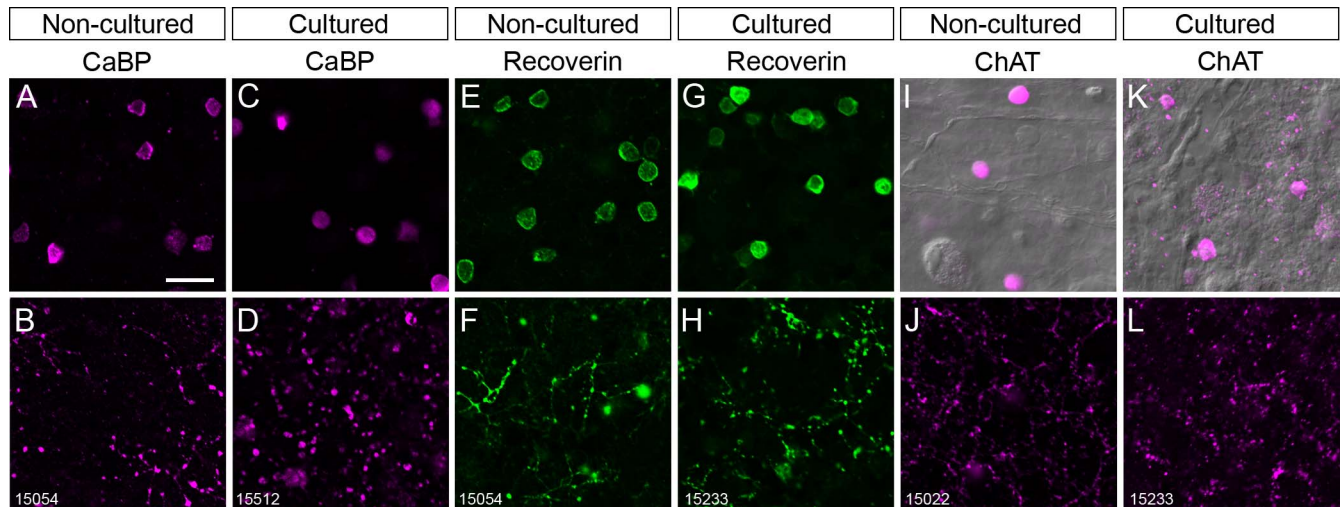


Figure 3. Comparison of bipolar and amacrine markers in cultured and noncultured flat mount preparations of human retina. (A–D) Confocal images of calbindin (CaBP) expressing bipolar cells. A shows the somas and B shows the axon terminals in noncultured retina, C shows the somas, and D the axon terminals in cultured retina. (E–H) Confocal images of recoverin expressing flat midget bipolar cells. E shows the somas and F shows the axon terminals in noncultured retina, G shows the somas and H shows the axon terminals in cultured retina. (I–L) Choline acetyl transferase (ChAT) immunoreactive displaced amacrine cells and their processes in noncultured (I, L) and cultured (K, L) retina. *Scale bar* = 20 μm in A (applies to all).

the postsynaptic sites to bipolar input.^{19,35,36} The piece of human retina was also processed with antibodies against the C-terminal binding protein 2 (CtBP2),³⁷ a marker for presynaptic ribbons (Fig. 4C) and the merged image shows that some of the PSD95-

GFP puncta are located close to CtBP2 immunoreactive puncta (arrows in Fig. 4D) consistent with the presence of synaptic connections. Similar results have been obtained in other species^{19,35,36} but will need to be analyzed more quantitatively in human retina.

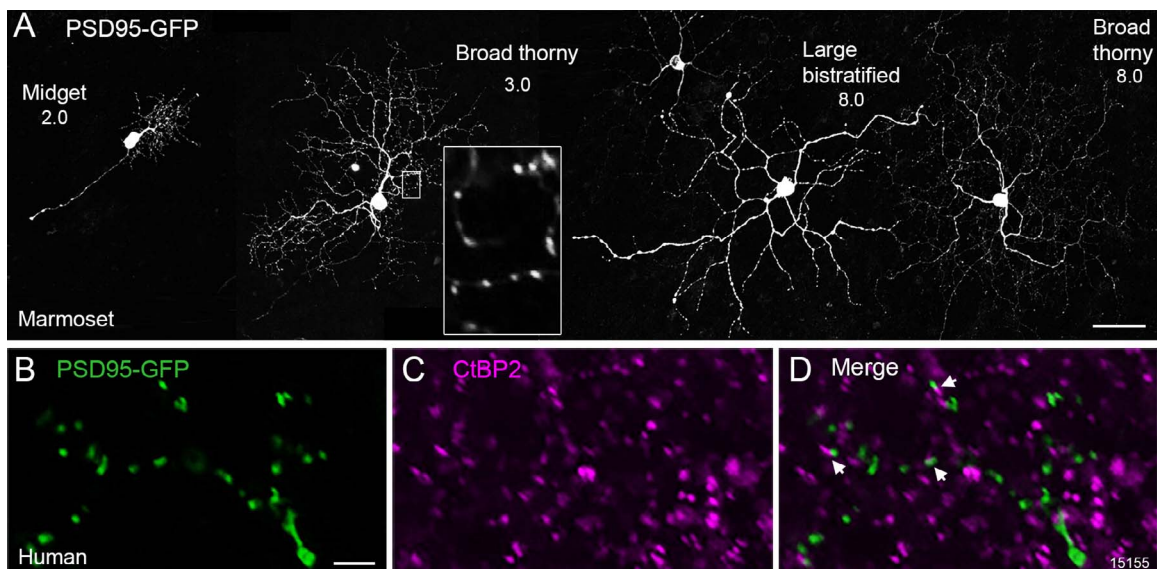


Figure 4. Expression of PSD95-GFP in retinal ganglion cells. (A) Marmoset retina: Photomontage of collapsed stacks of confocal images of ganglion cells labeled using particle-mediated gene transfection. Numbers indicate the distance from the fovea in millimeters for each cell. The *inset* represents a region of interest from the dendritic tree of the broad thorny ganglion cell shown on the left, showing the punctate expression of PSD95-GFP. (B–D) Human retina: Confocal images of the dendrites of a biolistic transfected ganglion cell processed with antibodies against the presynaptic ribbon protein CtBP2. *Arrows* point to PSD95-GFP puncta (*green*) associated with ganglion cell dendrites opposed to presynaptic ribbons (CtBP2, *magenta*). *Scale bar* = 50 μm in (A), 5 μm in B (applies to inset in A and B–D).

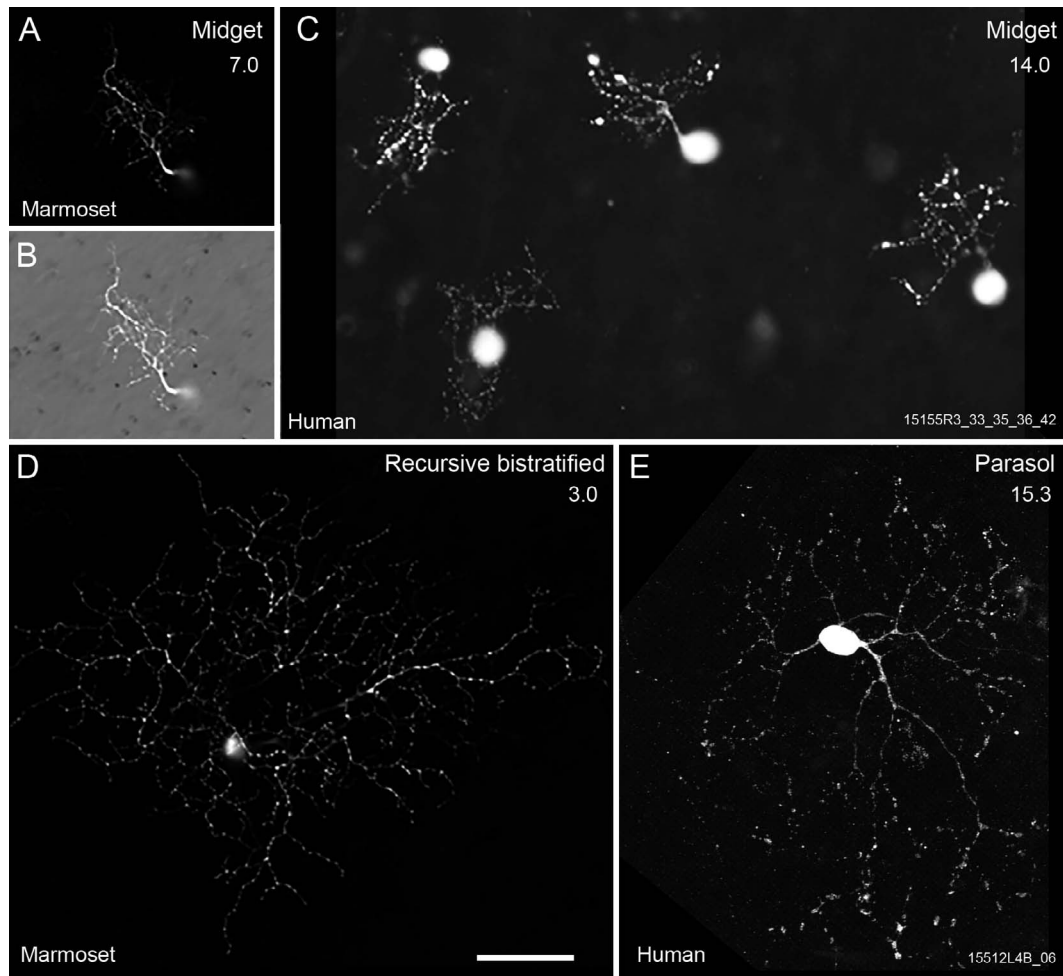


Figure 5. Expression of PSD95-GFP in ganglion cells labeled using particle-mediated gene transfection in marmoset (A, B, D) and human (C, E) retinas. The numbers indicate the eccentricities of the cells in millimeters. (A) Fluorescence micrograph of a midget ganglion cell imaged at the level of the inner plexiform layer. The same ganglion cell is shown in (B) together with differential interference contrast optics (DIC). (C) Fluorescence micrograph of midget ganglion cells in human retina, shown at the level of the dendrites. (D) Confocal projection of the dendritic tree of a recursive bistratified cell in marmoset retina. (E) Confocal projection of a parasol ganglion cell in human retina. Scale bar = 50 μm in C (applies to all).

The key factors for successful particle-mediated gene transfection in postmortem human retina were that (1) the retinas were processed within 15 hours of death, (2) the vitreous was completely removed, and (3) the explants were cultured for 3 to 4 days. When the time delay between death and immersion in Ames' medium exceeded 15 hours ($n = 11$ retinas), no particle-mediated labelling was observed. These retinas are not included in Table 1.

Figure 5 compares the expression of PSD95-GFP in midget ganglion cells of marmoset (Figs. 5A, 5B) and human retina (Fig. 5C). Due to their small dendritic field size, midget ganglion cells were more prone to overexpression of PSD95-GFP along their dendrites.²⁰ Further experiments are required to discern whether

shorter incubation times reduce overexpression of PSD-95 puncta along ganglion cell dendrites.

The distribution of the PSD95-GFP puncta along the dendrites of ganglion cells with larger dendritic fields is shown for a recursive bistratified cell in marmoset retina (Fig. 5D) and a parasol cell in human retina (Fig. 5E). As pointed out above, the PSD95-GFP puncta on the dendrites of ganglion cells in marmoset have a more uniform size and a more regular distribution.

In order to demonstrate that the ganglion cell layer in transfected and cultured retinas remains intact, some retinal pieces were processed with antibodies against RBPMS. Figure 6A shows a micrograph of such a retina and demonstrates that RBPMS labeling is present in cells with relatively large somas (presumed

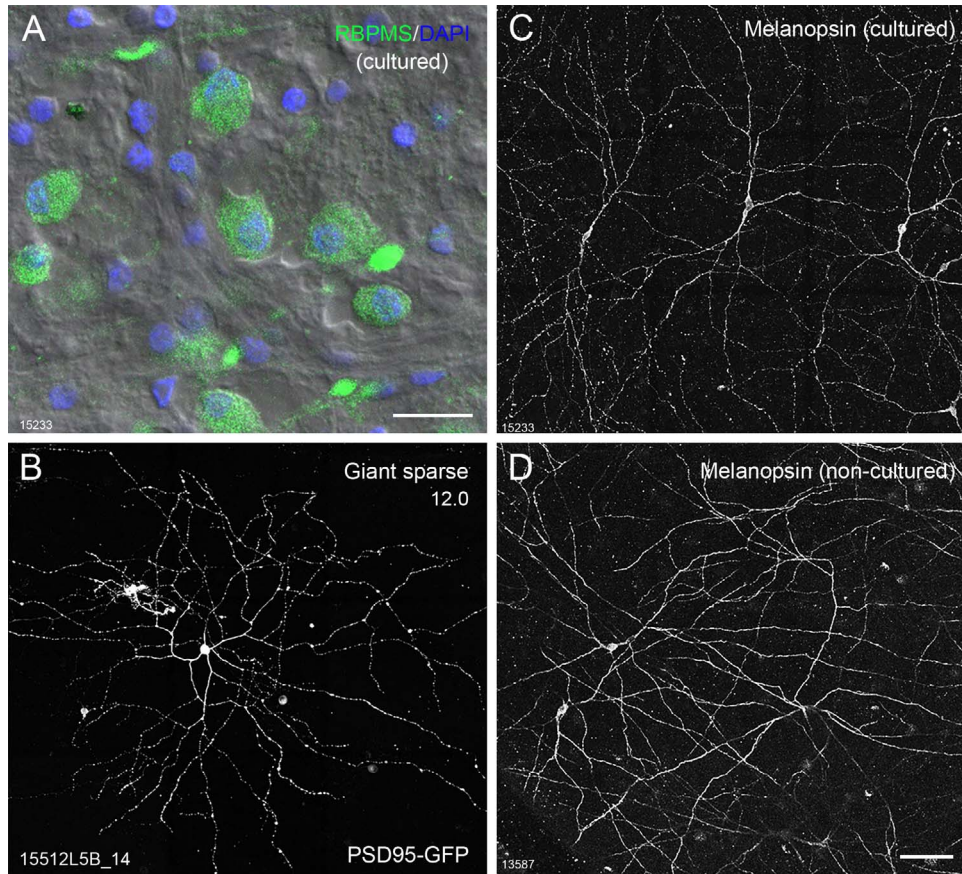


Figure 6. Human retina: ganglion cell labeling in cultured and noncultured retinas. (A) Confocal image of a flat mounted cultured human retina showing expression of RBPMS (green). The focus is on the ganglion cell layer. DAPI-labeled nuclei are shown in blue. (B) Maximum intensity projection of a giant sparse ganglion cell labeled using particle-mediated gene transfected PSD95-GFP. (C) Maximum intensity projection of a melanopsin-expressing ganglion cell in cultured retina. (D) Maximum intensity projection of a melanopsin-expressing ganglion cell in noncultured retina. Scale bar in A = 20 μm ; scale bar = 100 μm in D (applies to B–D).

ganglion cells), whereas unlabeled cells are thought to be displaced amacrine, glial, and endothelial cells.

Figure 6B shows a transfected ganglion cell with a very large sparse dendritic field (880 μm diameter) in human retina. This cell stratified mostly close to the ganglion cell layer but also had some dendrites close to the inner nuclear layer. Based on its large dendritic field size, we classified this cell as giant sparse cell.³⁸ Giant sparse cells are thought to be equivalent to melanopsin-expressing (intrinsically photosensitive) ganglion cells, which can be identified with antibodies against melanopsin.^{39,40} Here we applied these antibodies to cultured (Fig. 6C) and noncultured (Fig. 6D) human retinas. In both cases, the typical morphology of melanopsin-expressing ganglion cells can be distinguished, demonstrating that the morphology of intrinsically photosensitive ganglion cells is conserved in cultured retinas. Double labeling experiments would be required to confirm that

transfected giant sparse cells like the one shown in Figure 6B are indeed melanopsin expressing cells.

Classification of Ganglion Cell Types Labeled by Particle-Mediated Gene Transfection

In total, 126 transfected ganglion cells were analyzed in human retina. Examples of these cells are shown in Figures 5 to 8. Please note that the micrographs of the cells are maximum intensity projections from confocal stacks resulting in a less punctate appearance of the dendritic tree. The cells were derived from seven retinal pieces at eccentricities between 6 and 18 mm. Labelling near central retina was limited because the thick nerve fiber layer obstructed the passage of the bullets. Ganglion cells were classified based on the presence of an axon, dendritic field size relative to eccentricity, the morphology of their dendritic tree, and the stratification of their dendrites in the inner plexiform layer.^{40–47}

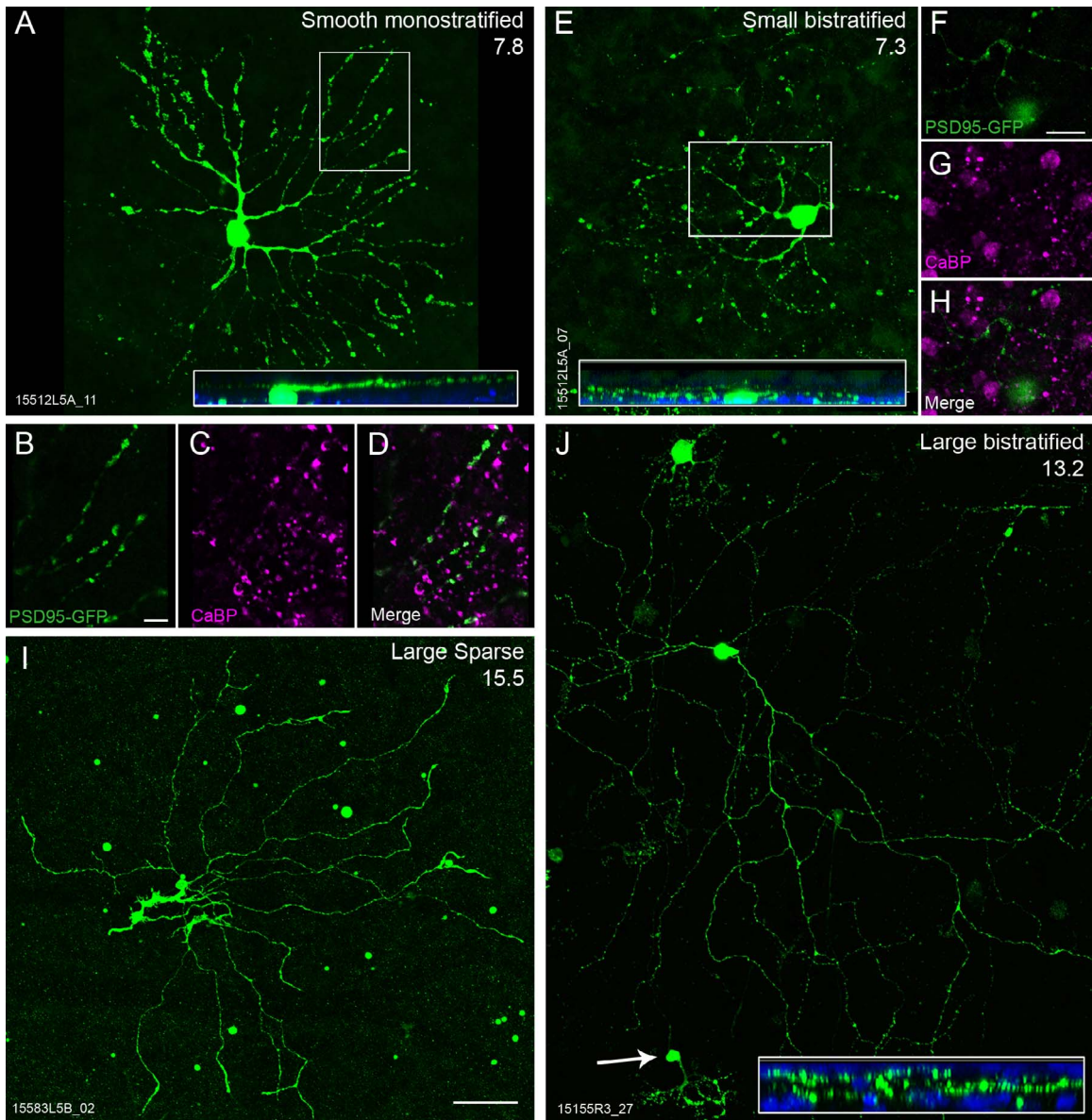


Figure 7. Human retina: confocal micrographs of ganglion cell types identified using particle-mediated gene transfection. The *insets* in A, E, and J show the stratification of the cells. *Blue* indicates DAPI labelling; the ganglion cell layer is located at the lower edge of the inset. (A) Collapsed stack of images of a smooth monostratified (SM) ganglion cell. (B–D) Single confocal planes showing the dendrites of the SM cell (*green*) co-stratifying with calbindin-labeled bipolar axon terminals (*magenta*). (E) Collapsed stack of images of a small bistratified ganglion cell. (F–H) Single confocal planes showing the dendrites of the SBS cell (*green*) with the calbindin-labeled bipolar axon terminals (*magenta*). (I) Collapsed stack of a large sparse ganglion cell. (J) Collapsed stack of a large bistratified (LBS) ganglion cell. A midget cell can also be seen in the lower left corner of the image (*arrow*). Eccentricity in millimeter is indicated in the *upper left-hand corner* for each cell. *Scale bar* = 10 μm in B (applies to B–D), 20 μm in F (applies to F–H), 50 μm in J (applies to A, E, I, J).

In total, 93 cells were classified as midget (73%), six cells were classified as parasol (5%), and eight cells were classified as small bistratified (6%). The remaining ganglion cells were widefield ganglion cell types (16%). [Figure 7](#) shows examples of labeled cells, [Figure 8](#) shows reconstructions of ganglion cell types

identified in this study, and [Figure 9](#) shows their dendritic field diameters with respect to eccentricity.

Midget ganglion cells have the smallest dendritic field size at all locations, a single primary dendrite, and a small soma that is positioned away from the dense dendritic tree ([Figs. 5A–C, 7J, 8](#)). Parasol cells have a

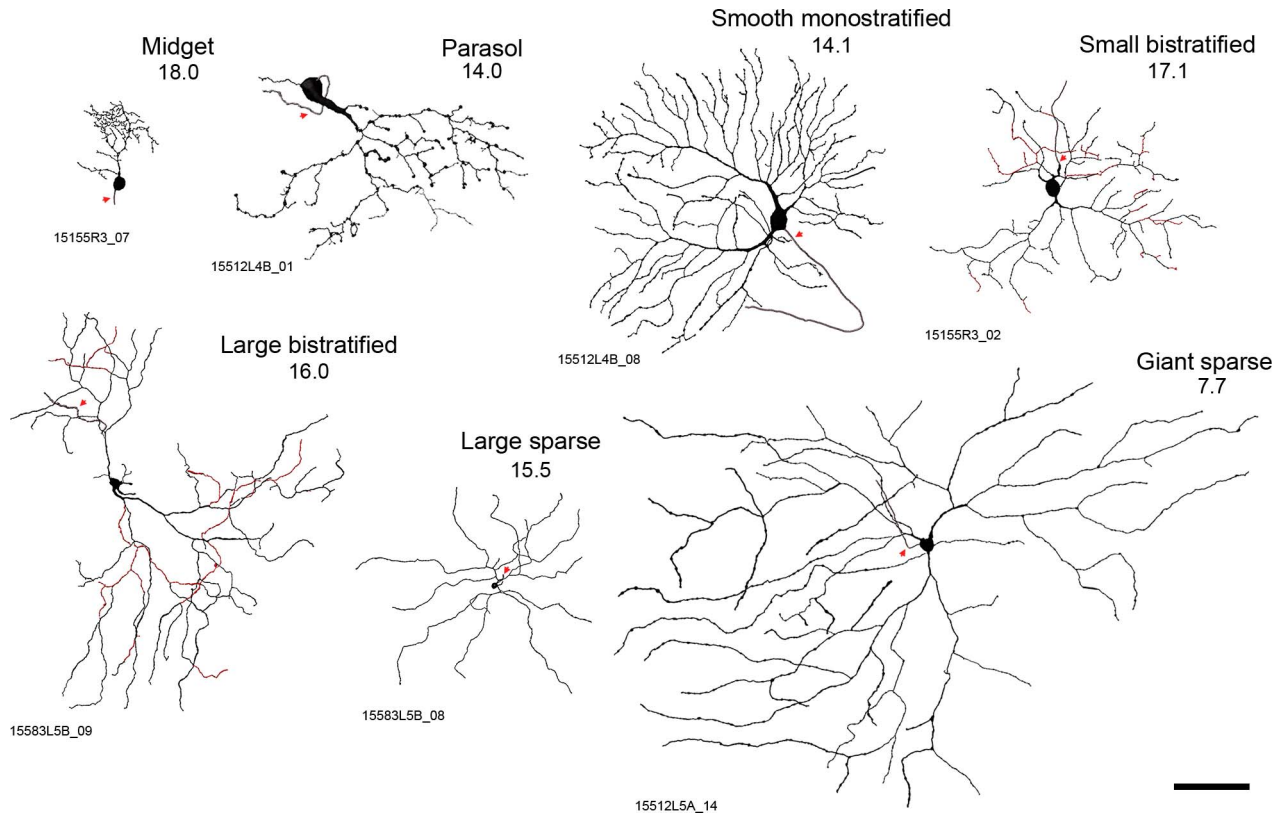


Figure 8. Human retina: reconstructions of ganglion cell types labelled using particle-mediated gene transfection. The numbers indicate the distance from the fovea in millimeters. *Arrows* point to axons; the outer dendrites of bistratified cells are shown in *red*. *Scale bar* = 100 μm .

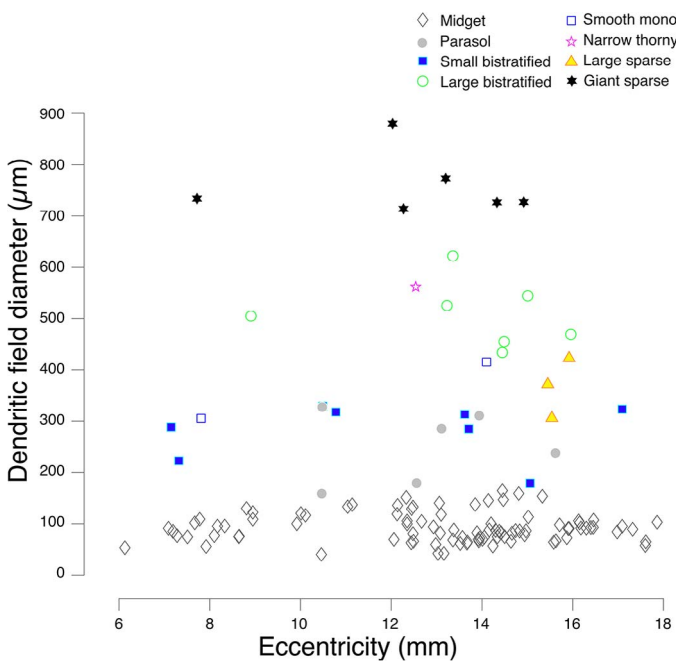


Figure 9. Human retina: *Scatter plot* showing dendritic field diameter as a function of retinal eccentricity for ganglion cells labeled using particle-mediated gene transfection.

large soma and thick primary dendrites (Figs. 5E, 8). Although parasol ganglion cells in our samples exhibited typical characteristics and dendritic field diameter, the dendritic tree was weakly labeled, asymmetrical in some cases, and sparser than expected. Small bistratified cells have a sparse bistratified dendritic tree and a dendritic field size comparable to parasol cells. Examples of small bistratified cells are shown in Figs. 7E and 8; they have a comparatively large inner dendritic tree and a small outer dendritic tree. The outer dendritic tree stratifies slightly sclerad relative to the terminals of calbindin labeled DB3a cells (Figs. 7F–7H) in stratum 3 and the inner dendritic tree stratifies in stratum 5 of the inner plexiform layer.

Widefield ganglion cells included smooth monostratified, large bistratified, narrow thorny, sparse, and giant sparse ganglion cells. Smooth monostratified cells ($n = 2$) have smooth, straight dendrites that radiate from the soma in the center of the dendritic field (Figs. 7A, 8). Their dendrites stratified in the OFF sublamina at the same level as DB3a axon terminals (Figs. 7B–7D). Large sparse cells ($n = 3$) had dendritic trees that were consistently smaller than

giant sparse cells but stratified at similar levels of the inner plexiform layer. An example of an inner stratifying large sparse cell is shown in [Figure 7I](#). Large bistratified cells ($n = 7$; [Fig. 7J](#)), stratified at the same level as the small bistratified cells, in strata 3 and 5 of the inner plexiform layer (inset in [Fig. 7J](#)). In addition to the giant sparse cell shown above ([Fig. 4B](#)), we found five other cells with this morphology and dendritic field size ([Figs. 8, 9](#)), four cells stratified close to the inner nuclear, and two cells stratified close to the ganglion cell layer.

Discussion

The main finding of this study is that particle-mediated gene transfection can be used to label ganglion cells in organotypic cultured postmortem human retina. We also show that transfected retinal tissue can be processed with bipolar markers, which will enable the study of the synaptic input to labeled ganglion cells¹⁹ in future studies.

The morphology of transfected ganglion cells from freshly enucleated marmoset retinas was similar to the human retinas with less than 15 hours postmortem delay. However, there were discrepancies with respect to the quality of the expression of PSD95-GFP. These differences between marmoset and human retina are most likely due to the differences in the preparation and treatment of the eyes and retina prior to biolistic transfection and organotypic culture. Marmoset eyes were perfused with a chilled sucrose-based solution, enucleated, and then placed immediately into Ames' medium, while human eyes were stored in CO₂ Independent medium for up to 9 hours prior to being placed into Ames' medium. A reduced time window between death and gene transfection is likely to improve results in human retinal explants.

Ganglion cells identified in this study largely resembled those identified previously in humans using a variety of other methods.^{40,41,45,46,48} Similarly, previous studies in animals have shown that retinal ganglion cells labeled by particle-mediated gene transfection^{17,20,35} have comparable morphology to that detected with other methods.^{38,47,49–53} However, we found differences in the proportions of cells labeled in human retina compared to previous studies. Parasol ganglion cells were found in much lower proportions than expected and had sparser dendritic trees than previously reported.^{41,42} In macaque monkey, cells with large axon diameters have been found to be more susceptible to glaucoma.⁵⁴ Whether our findings in

human suggest that parasol cells are more susceptible to postmortem changes needs further investigation.

As discussed previously^{20,55} biolistic labelling is probably somewhat biased, but it is unlikely that it is biased toward a particular soma or dendritic field size because labelling by particle-mediated gene transfection depends on the particles effectively reaching the cell nucleus and on the ability of the cell to transcribe and express the transgene. In marmoset retina, thorny ganglion cells comprised a large proportion of the transfected cells,^{17,20} but these cells are near absent in the human samples. It is possible that the dense dendritic tree of thorny ganglion cells is less likely to express PSD95-GFP in postmortem cultures, but this needs further investigation. Another interesting result is that we found six giant sparse cells (presumed melanopsin expressing cells) although these cells make up less than 1% of the retinal ganglion cell population.^{40,56} Previous studies have shown that melanopsin-expressing ganglion cells are more resistant to neurodegeneration compared to other ganglion cell types after optic nerve injury.^{57,58} Thus, it is possible that melanopsin-expressing cells are more easily transfected than other ganglion cell types. Alternatively, the transfected cells classified as giant sparse could include a yet to be described ganglion cell type.

Our study shows that expression of ganglion and glial cell markers is comparable in cultured and noncultured retinas. These markers are important indicators of the preservation of retinal architecture^{13,22,59} since protein expression in these cell types is altered in response to injury.^{60,61} Previous studies have shown that degeneration of the retina becomes evident after a culture period longer than 3 days.^{14,35,62} Other studies have cultured human retinas for several weeks to achieve transduction of adeno-associated viral vectors,^{10,11} but the viability of ganglion cells in these retinas was not systematically assessed.

The present study followed a protocol first applied to primate retina by Moritoh et al.¹⁷ who used Ames' medium supplemented with normal horse serum and antibiotics.^{2,17} Ames' medium is known to facilitate the survival of retinal neurons for up to 6 days for electrophysiological recordings.^{2,63} Previous studies in murine culture systems excluded serum from the culture media because much of its composition is unknown.^{8,64,65} Studies on rat retina determined that serum-free defined culture media containing B27/N2 supplements extended explant viability by at least 1 week,⁵⁹ but in human retina the survival of neurons decreased after 2 days in serum-free medium.¹³ It is unclear whether the use of serum had any adverse or

positive effect on our samples of human retina, but serum was also included in the culture of marmoset retina with excellent results.

The applications of biolistic transfer have been demonstrated previously in mouse,⁶⁶ rabbit,^{2,35,51} and marmoset^{17–19} retinas. The feasibility of this method in human retina allows for a broader use of postmortem donor tissue. Particle-mediated gene transfer is relatively rapid, requires little maintenance, and provides a system within which multiple parameters can be controlled and easily manipulated. Biolistic labelling can be carried out using combinations of plasmids targeting different genes in the same preparation. Ultimately, the system described here holds potential for clinical translation in allowing genetic manipulation, electrophysiological recording, and evaluation of changes in specific cell types in human retinal tissue.

Acknowledgments

We thank Rajnesh Devasahayam and Meidong Zhu from the Lions NSW Eye Bank at Sydney Eye Hospital for making human donor eyes available. Marmoset tissue was obtained with the help of Alexander Pietersen, Natalie Zeater, and Paul Martin. We thank Calvin Eiber for designing and printing the filter stands used in organotypic culture. We are also grateful to Amane Koizumi and Rachel Wong for their expert advice and to Arzu Demir for excellent technical assistance.

Supported by Research Training Program Stipend (RAM); Ophthalmology and Vision Science PhD Scholarship by the Save Sight Institute/Sydney Eye Hospital Foundation (RAM); National Health & Medical Research Council (NHMRC) Project grant (1123418 to UG); Australian Research Council Centre of Excellence for Integrative Brain Function (ARC Centre Grant CE140100007 to UG); Claffy Foundation (SCSL); U.G. is a Sydney Medical School Foundation Fellow.

Disclosure: **R.A. Masri**, None; **S.C.S. Lee**, None; **M.C. Madigan**, None; **U. Grünert**, None

References

1. Binley KE, Ng WS, Barde YA, Song B, Morgan JE. Brain-derived neurotrophic factor prevents

- dendritic retraction of adult mouse retinal ganglion cells. *Eur J Neurosci*. 2016;44:2028–2039.
2. Koizumi A, Zeck G, Ben Y, Masland RH, Jakobs TC. Organotypic culture of physiologically functional adult mammalian retinas. *PLoS One*. 2007; 2:e221.
3. Pérez-León J, Frech MJ, Schröder E Jr, et al. Spontaneous synaptic activity in an organotypic culture of the mouse retina. *Invest Ophthalmol Vis Sci*. 2003;44:1376–1387.
4. Pinzón-Duarte G, Kohler K, Arango-González B, Guenther E. Cell differentiation, synaptogenesis, and influence of the retinal pigment epithelium in a rat neonatal organotypic retina culture. *Vision Res*. 2000;40:3455–3465.
5. Ruscher K, Rzczinski S, Thein E, et al. Neuroprotective effects of the β -carboline abcarnil studied in cultured cortical neurons and organotypic retinal cultures. *Neuropharmacology*. 2007;52:1488–1495.
6. White AJ, Heller JP, Leung J, Tassoni A, Martin KR. Retinal ganglion cell neuroprotection by an angiotensin II blocker in an ex vivo retinal explant model. *J Renin Angiotensin Aldosterone Syst*. 2015;16:1193–1201.
7. Johnson TV, Oglesby EN, Steinhart MR, Cone-Kimball E, Jefferys J, Quigley HA. Time-lapse retinal ganglion cell dendritic field degeneration imaged in organotypic retinal explant culture. *Invest Ophthalmol Vis Sci*. 2016;57:253–264.
8. Valdés J, Trachsel-Moncho L, Sahaboglu A, et al. Organotypic retinal explant cultures as in vitro alternative for diabetic retinopathy studies. *ALTEX*. 2016;33:459.
9. Manabe S-I, Kashii S, Honda Y, Yamamoto R, Katsuki H, Akaike A. Quantification of axotomized ganglion cell death by explant culture of the rat retina. *Neurosci Lett*. 2002;334:33–36.
10. Fradot M, Busskamp V, Forster V, et al. Gene therapy in ophthalmology: validation on cultured retinal cells and explants from postmortem human eyes. *Hum Gene Ther*. 2010;22:587–593.
11. Busskamp V, Duebel J, Balya D, et al. Genetic reactivation of cone photoreceptors restores visual responses in retinitis pigmentosa. *Science*. 2010;329:413–417.
12. Sengupta A, Chaffiol A, Macé E, et al. Red-shifted channel rhodopsin stimulation restores light responses in blind mice, macaque retina, and human retina. *EMBO Mol Med*. 2016;8:1248–1264.
13. Niyadurupola N, Sidaway P, Osborne A, Broadway DC, Sanderson J. The development of human organotypic retinal cultures (HORCs) to

- study retinal neurodegeneration. *Br J Ophthalmol*. 2011;95:720–726.
14. Fernandez-Bueno I, Fernández-Sánchez L, Gayoso MJ, García-Gutierrez MT, Pastor JC, Cuenca N. Time course modifications in organotypic culture of human neuroretina. *Exp Eye Res*. 2012;104:26–38.
 15. Moritoh S, Tanaka KF, Jouhou H, Ikenaka K, Koizumi A. Organotypic tissue culture of adult rodent retina followed by particle-mediated acute gene transfer in vitro. *PLoS One*. 2010;5:e12917.
 16. Kerschensteiner D, Morgan JL, Parker ED, Lewis RM, Wong RO. Neurotransmission selectively regulates synapse formation in parallel circuits in vivo. *Nature*. 2009;460:1016.
 17. Moritoh S, Komatsu Y, Yamamori T, Koizumi A. Diversity of retinal ganglion cells identified by transient GFP transfection in organotypic tissue culture of adult marmoset monkey retina. *PLoS One*. 2013;8:e54667.
 18. Percival KA, Koizumi A, Masri RA, Buzás P, Martin PR, Grünert U. Identification of a pathway from the retina to koniocellular layer K1 in the lateral geniculate nucleus of marmoset. *J Neurosci*. 2014;34:3821–3825.
 19. Masri RA, Percival KA, Koizumi A, Martin PR, Grünert U. Connectivity between the OFF bipolar type DB3a and six types of ganglion cell in the marmoset retina. *J Comp Neurol*. 2016;524:1839–1858.
 20. Masri RA, Percival KA, Koizumi A, Martin PR, Grünert U. Survey of retinal ganglion cell morphology in marmoset. *J Comp Neurol*. 2019;527:236–258.
 21. Zhang C, Yu WQ, Hoshino A, et al. Development of ON and OFF cholinergic amacrine cells in the human fetal retina. *J Comp Neurol*. 2019;527:174–186.
 22. Di Lauro S, Rodriguez-Crespo D, Gayoso MJ, et al. A novel coculture model of porcine central neuroretina explants and retinal pigment epithelium cells. *Mol Vis*. 2016;22:243.
 23. Kaempfer S, Walter P, Salz AK, Thumann G. Novel organotypic culture model of adult mammalian neurosensory retina in co-culture with retinal pigment epithelium. *J Neurosci Methods*. 2008;173:47–58.
 24. Pietersen AN, Ward PD, Hagger-Vaughan N, Wiggins J, Jefferys JG, Vreugdenhil M. Transition between fast and slow gamma modes in rat hippocampus area CA1 in vitro is modulated by slow CA3 gamma oscillations. *J Physiol*. 2014;592:605–620.
 25. O'Brien JA, Lummis SC. Diolistic labeling of neuronal cultures and intact tissue using a hand-held gene gun. *Nat Protoc*. 2006;1:1517.
 26. Schindelin J, Arganda-Carreras I, Frise E, et al. Fiji: an open-source platform for biological-image analysis. *Nat Methods*. 2012;9:676.
 27. Haverkamp S, Haeseleer F, Hendrickson A. A comparison of immunocytochemical markers to identify bipolar cell types in human and monkey retina. *Vis Neurosci*. 2003;20:589–600.
 28. Puthussery T, Venkataramani S, Gayet-Primo J, Smith RG, Taylor WR. NaV1.1 channels in axon initial segments of bipolar cells augment input to magnocellular visual pathways in the primate retina. *J Neurosci*. 2013;33:16045–16059.
 29. Milam AH, Dacey DM, Dizhoor AM. Recoverin immunoreactivity in mammalian cone bipolar cells. *Vis Neurosci*. 1993;10:1–12.
 30. Rodieck R, Marshak D. Spatial density and distribution of choline acetyltransferase immunoreactive cells in human, macaque, and baboon retinas. *J Comp Neurol*. 1992;321:46–64.
 31. Lee S, Weltzien F, Madigan MC, Martin PR, Grünert U. Identification of AII amacrine, displaced amacrine, and bistratified ganglion cell types in human retina with antibodies against calretinin. *J Comp Neurol*. 2016;524:39–53.
 32. de Souza CF, Nivison-Smith L, Christie DL, et al. Macromolecular markers in normal human retina and applications to human retinal disease. *Exp Eye Res*. 2016;150:135–148.
 33. Kwong JM, Caprioli J, Piri N. RNA binding protein with multiple splicing: a new marker for retinal ganglion cells. *Invest Ophthalmol Vis Sci*. 2010;51:1052–1058.
 34. Rodriguez AR, Müller S, Pérez L, Brecha NC. The RNA binding protein RBPMS is a selective marker of ganglion cells in the mammalian retina. *J Comp Neurol*. 2014;522:1411–1443.
 35. Jakobs TC, Koizumi A, Masland RH. The spatial distribution of glutamatergic inputs to dendrites of retinal ganglion cells. *J Comp Neurol*. 2008;510:221–236.
 36. Bleckert A, Schwartz GW, Turner MH, Rieke F, Wong RO. Visual space is represented by non-matching topographies of distinct mouse retinal ganglion cell types. *Curr Biol*. 2014;24:310–315.
 37. Schmitz F, Königstorfer A, Südhof TC. RIBEYE, a component of synaptic ribbons: a protein's journey through evolution provides insight into synaptic ribbon function. *Neuron*. 2000;28:857–872.
 38. Rodieck RW, Watanabe M. Survey of the morphology of macaque retinal ganglion cells that project to the pretectum, superior colliculus,

- and parvicellular laminae of the lateral geniculate nucleus. *J Comp Neurol*. 1993;338:289–303.
39. Dacey DM, Liao H-W, Peterson BB, et al. Melanopsin-expressing ganglion cells in primate retina signal colour and irradiance and project to the LGN. *Nature*. 2005;433:749.
 40. Nasir-Ahmad S, Lee S, Martin PR, Grünert U. Melanopsin-expressing ganglion cells in human retina: morphology, distribution, and synaptic connections. *J Comp Neurol*. 2019;527:312–327.
 41. Rodieck RW, Binmoeller K, Dineen J. Parasol and midget ganglion cells of the human retina. *J Comp Neurol*. 1985;233:115–132.
 42. Dacey DM, Petersen MR. Dendritic field size and morphology of midget and parasol ganglion cells of the human retina. *Proc Natl Acad Sci*. 1992;89:9666–9670.
 43. Dacey DM. The mosaic of midget ganglion cells in the human retina. *J Neurosci*. 1993;13:5334–5355.
 44. Dacey DM. Morphology of a small-field bistratified ganglion cell type in the macaque and human retina. *Vis Neurosci*. 1993;10:1081–1098.
 45. Peterson BB, Dacey DM. Morphology of wide-field, monostратified ganglion cells of the human retina. *Vis Neurosci*. 1999;16:107–120.
 46. Peterson BB, Dacey DM. Morphology of wide-field bistratified and diffuse human retinal ganglion cells. *Vis Neurosci*. 2000;17:567–578.
 47. Dacey DM, Peterson BB, Robinson FR, Gamlin PD. Fireworks in the primate retina: in vitro photodynamics reveals diverse LGN-projecting ganglion cell types. *Neuron*. 2003;37:15–27.
 48. Kolb H, Linberg KA, Fisher SK. Neurons of the human retina: a Golgi study. *J Comp Neurol*. 1992;318:147–187.
 49. Perry V, Cowey A. Retinal ganglion cells that project to the superior colliculus and pretectum in the macaque monkey. *Neuroscience*. 1984;12:1125–1137.
 50. Ghosh KK, Goodchild AK, Sefton AE, Martin PR. Morphology of retinal ganglion cells in a new world monkey, the marmoset *Callithrix jacchus*. *J Comp Neurol*. 1996;366:76–92.
 51. Rockhill RL, Daly FJ, MacNeil MA, Brown SP, Masland RH. The diversity of ganglion cells in a mammalian retina. *J Neurosci*. 2002;22:3831–3843.
 52. Yamada ES, Bordt AS, Marshak DW. Wide-field ganglion cells in macaque retinas. *Vis Neurosci*. 2005;22:383–393.
 53. Szmajda BA, Grünert U, Martin PR. Retinal ganglion cell inputs to the koniocellular pathway. *J Comp Neurol*. 2008;510:251–268.
 54. Glovinsky Y, Quigley H, Dunkelberger G. Retinal ganglion cell loss is size dependent in experimental glaucoma. *Invest Ophthalmol Vis Sci*. 1991;32:484–491.
 55. Kong JH, Fish DR, Rockhill RL, Masland RH. Diversity of ganglion cells in the mouse retina: unsupervised morphological classification and its limits. *J Comp Neurol*. 2005;489:293–310.
 56. Liao HW, Ren X, Peterson BB, et al. Melanopsin-expressing ganglion cells on macaque and human retinas form two morphologically distinct populations. *J Comp Neurol*. 2016;524:2845–2872.
 57. La Morgia C, Ross-Cisneros FN, Sadun AA, et al. Melanopsin retinal ganglion cells are resistant to neurodegeneration in mitochondrial optic neuropathies. *Brain*. 2010;133:2426–2438.
 58. de Sevilla Müller LP, Sargoy A, Rodriguez AR, Brecha NC. Melanopsin ganglion cells are the most resistant retinal ganglion cell type to axonal injury in the rat retina. *PLoS One*. 2014;9:e93274.
 59. Johnson TV, Martin KR. Development and characterization of an adult retinal explant organotypic tissue culture system as an in vitro intraocular stem cell transplantation model. *Invest Ophthalmol Vis Sci*. 2008;49:3503–3512.
 60. Pattamatta U, McPherson Z, White A. A mouse retinal explant model for use in studying neuroprotection in glaucoma. *Exp Eye Res*. 2016;151:38–44.
 61. Bringmann A, Pannicke T, Grosche J, et al. Müller cells in the healthy and diseased retina. *Prog Retin Eye Res*. 2006;25:397–424.
 62. Müller B, Wagner F, Lorenz B, Stieger K. Organotypic cultures of adult mouse retina: morphologic changes and gene expression. *Invest Ophthalmol Vis Sci*. 2017;58:1930–1940.
 63. Ames A, Nesbett F. In vitro retina as an experimental model of the central nervous system. *J Neurochem*. 1981;37:867–877.
 64. Caffè A, Ahuja P, Holmqvist B, et al. Mouse retina explants after long-term culture in serum free medium. *J Chem Neuroanat*. 2002;22:263–273.
 65. Romijn H, De Jong B, Ruijter J. A procedure for culturing rat neocortex explants in a serum-free nutrient medium. *J Neurosci Methods*. 1988;23:75–83.
 66. Morgan JL, Soto F, Wong RO, Kerschensteiner D. Development of cell type-specific connectivity patterns of converging excitatory axons in the retina. *Neuron*. 2011;71:1014–1021.